MOLECULAR IMAGING AND BIOLOGY

Mol Imaging Biol (2021) 23:127–138
DOI: 10.1007/s11307-020-01540-6

Published Online: 14 September 2020

WMIS World Molecular Imaging Society
esmi European Society for Molecular Imaging

Check for updates

RESEARCH ARTICLE

Imaging Butyrylcholinesterase in Multiple Sclerosis

M. W. D. Thorne,[1,2] M. K. Cash,[1] G. A. Reid,[1] D. E. Burley,[1] D. Luke,[1] I. R. Pottie,[3,4] S. Darvesh[1,2,3]

[1]*Department of Medical Neuroscience, Dalhousie University, Halifax, NS, Canada*
[2]*Department of Medicine (Neurology), Dalhousie University, Halifax, NS, Canada*
[3]*Department of Chemistry and Physics, Mount Saint Vincent University, Halifax, NS, Canada*
[4]*Department of Chemistry, Saint Mary's University, Halifax, NS, Canada*

Abstract

Purpose: Molecular imaging agents targeting butyrylcholinesterase (BChE) have shown promise in other neurodegenerative disorders and may have utility in detecting changes to normal appearing white matter in multiple sclerosis (MS). BChE activity is present in white matter and localizes to activated microglia associated with MS lesions. The purpose of this study was to further characterize changes in the cholinergic system in MS pathology, and to explore the utility of BChE radioligands as potential diagnostic and treatment monitoring agents in MS.

Procedure: Cortical and white matter lesions were identified using myelin staining, and lesions were classified based on microglial activation patterns. Adjacent brain sections were used for cholinesterase histochemistry and *in vitro* autoradiography using phenyl 4-[^{123}I]-iodophenylcarbamate (^{123}I-PIP), a previously described small-molecule cholinesterase-binding radioligand.

Results: BChE activity is positively correlated with microglial activation in white matter MS lesions. There is no alteration in cholinesterase activity in cortical MS lesions. ^{123}I-PIP autoradiography revealed uptake of radioactivity in normal white matter, absence of radioactivity within demyelinated MS lesions, and variable uptake of radioactivity in adjacent normal-appearing white matter.

Conclusions: BChE imaging agents have the potential to detect MS lesions and subtle pathology in normal-appearing white matter in postmortem MS brain tissue. The possibility of BChE imaging agents serving to supplement current diagnostic and treatment monitoring strategies should be evaluated.

Key words: Multiple sclerosis, Butyrylcholinesterase, Autoradiography, Molecular imaging

Introduction

Multiple sclerosis (MS) is a chronic immune-mediated inflammatory and neurodegenerative disease of the central nervous system (CNS). The etiopathogenesis of MS is complex, and involves an unknown trigger causing inflammatory demyelinating white matter lesions, cortical demyelination, and accelerated brain and spinal cord atrophy [1–5]. MS can affect vision, strength, sensation, coordination,

Electronic supplementary material The online version of this article (https://doi.org/10.1007/s11307-020-01540-6) contains supplementary material, which is available to authorized users.

Correspondence to: S. Darvesh; *e-mail:* sultan.darvesh@dal.ca

mobility, and cognition. A single demyelinating attack is termed a clinically isolated syndrome (CIS), and in individuals with a CIS, the risk of progression to MS ranges from 42 to 82 %, [6, 7]. There are three main subtypes of MS, including relapsing-remitting (RRMS), primary progressive (PPMS), and secondary progressive (SPMS), and these subtypes are named for the presence or absence of clinical relapses and disability progression [8].

Diagnosis of MS requires a clinical assessment and a magnetic resonance imaging (MRI) scan of the brain to help confirm the location of disease activity and rule out disorders that can mimic MS [9, 10]. MRI has brought several benefits to the management of MS, and is used to monitor disease activity and treatment response [11, 12]. A standard MRI protocol [12] can accurately predict the transition from CIS to MS with a sensitivity ranging from 72 to 82 % and a specificity ranging from 48 to 55 %, depending on the criteria used [13, 14]. Although MRI can detect demyelination, limitations of this imaging modality include its inability to detect specific underlying pathologies like immune cell infiltration and axonal degeneration, as well as the inability to identify changes to normal-appearing white matter (NAWM) [15]. NAWM changes are more widespread and occur earlier in the disease process than previously appreciated [3, 16]. Although MRI remains the gold standard in the diagnosis and management of MS, the ability to identify specific pathological changes to NAWM could lead to earlier diagnosis and better treatment monitoring of the disease.

The cholinergic system is a network of neurons, glia, and immune cells that use acetylcholine (ACh) to carry out physiologic processes [17]. ACh is an excitatory neurotransmitter that is synthesized from choline and acetyl-CoA by choline acetyltransferase (ChAT). Acetylcholinesterase (AChE) and butyrylcholinesterase (BChE) are regulating enzymes of this neurotransmitter [17]. AChE-knockout mice survive, thus indicating a significant role for BChE in modulating cholinergic neurotransmission [18, 19]. ACh binds to two families of cholinergic receptors, named for their relative affinity for nicotine (nAChR) or muscarine (mAChR) [17].

In the CNS, ChAT-positive cholinergic neurons are located in distinct nuclei of the basal forebrain (nucleus basalis of Meynert) and brainstem (pedunculopontine and laterodorsal tegmental nuclei), and have projections throughout the cortex and to select subcortical structures *via* the medial and lateral cholinergic pathways [20–22]. AChE-positive neurons are observed throughout the cerebral and cerebellar cortices, and within the basal ganglia, thalamus, hypothalamus, hippocampus, and amygdala, whereas white matter AChE-positive processes are restricted to the medial and lateral cholinergic pathways [21, 22]. In comparison, BChE-positive neurons are restricted to distinct populations in the amygdala, hippocampal formation, and thalamus [23, 24]. BChE activity is observed at higher levels in normal white matter compared to AChE, and localizes in blood vessels and glial cells [19, 25].

BChE has been identified as an important enzyme in the pathogenesis of many neurological diseases, most notably in the association with β-amyloid plaques in Alzheimer's disease (AD) [26–30]. Molecular imaging technologies, including positron emission tomography (PET) and single-photon emission computed tomography (SPECT), have been used to visualize abnormal BChE accumulation in the cerebral cortex of a familial AD mouse model, providing proof -of- concept for this technology [30–32]. The development of these ligands as imaging biomarkers to aid in the diagnosis of AD requires further evaluation. Phenyl 4-iodophenylcarbamate (PIP) was developed as a ligand to bind to cholinesterases with a high affinity for BChE, and demonstrates covalent substrate binding and inhibitor properties, making it biologically relevant for further study [33].

Cholinergic neurotransmission has many putative links to MS pathogenesis. BChE activity is altered in MS plaques and adjacent white matter [25]. This change in BChE activity may be significant, as BChE has been shown to hydrolyze long-chain acyl groups such as those found in proteolipid protein (PLP), a major myelin component [34]. This could result in myelin decompaction, exposing sequestered myelin antigens to the immune system and accelerating epitope spread, perpetuating the autoimmune response [34, 35].

We hypothesize that BChE imaging agents are an ideal target for preclinical evaluation to detect subtle changes in NAWM, as BChE has been identified as a putative enzyme in the pathogenesis of MS and is found at high levels in the white matter. The possibility of BChE imaging agents serving to supplement current diagnostic and treatment monitoring strategies should be evaluated. To test this hypothesis, histochemical and immunohistochemical techniques were used to classify MS lesions and to analyze the relationships between BChE, AChE, and neuroinflammatory markers in MS compared with normal brain tissues, including white and gray matter lesions and surrounding NAWM. Additionally, we evaluated the utility of a BChE imaging agent to distinguish normal white matter, NAWM, and demyelinated MS lesions in MS brain tissues, using *in vitro* autoradiography with a synthetic radioligand for BChE, as a proof of concept to enable future *in vivo* experiments.

Materials and Methods

Brain Tissues

A total of 11 brain tissue blocks from five MS cases and 15 tissue blocks from five age- and sex-matched control cases were obtained from the Maritime Brain Tissue Bank (Dalhousie University, Halifax, Nova Scotia, Canada) following approval from the Nova Scotia Health Authority Research Ethics Board. Demographic data is summarized in Table 1. The normal cases did not have a history of neurological illness, and the neuropathological report excluded any other vascular,

neoplastic, demyelinating, or neurodegenerative pathology. The postmortem interval for all cases ranged between 7 and 82 h. Brains had previously been cut in 1–2-cm coronal slabs after immersion fixation in 10 % formalin in 0.1 M phosphate buffer (PB), pH 7.4, at 4 °C for up to 5 days. Brain slabs were cryoprotected using graduated concentrations of sucrose up to a target of 40 % and then stored in 40 % sucrose in 0.1 M PB with 0.6 % sodium azide until use. Blocks that contained macroscopic MS plaques were selected from slabs including orbitofrontal and occipital cortices. Corresponding areas were obtained from control brain slabs for comparison. Blocks were cut into 50 μm-thick serial sections using a Leica SM2000R microtome with a Physitemp freezing stage. Sections were then stored frozen at – 20 °C in 40 % sucrose in 0.1 M PB until use.

Histochemical Staining

Histochemical staining for AChE and BChE was carried out using a modified Karnovsky-Roots method as previously described [36]. The details of the methodology and control experiments are provided in the Electronic Supplementary Material (ESM).

Adjacent sections were stained for luxol fast blue (LFB) to visualize myelin and counterstained with cresyl violet (CV) to visualize nuclear cytoarchitecture. All reagents were purchased from Sigma-Aldrich. Sections were mounted on slides, air-dried, dehydrated in a graded series of aqueous ethanol (70%, 95%, 100%), cleared in xylene, rehydrated to 95 % ethanol, and incubated (2 h) in a 1 % solution of LFB in 95 % ethanol at 60 °C. Slides were washed (1 min) in 95 % ethanol and again (1 min) in distilled water, to remove excess LFB dye. Slides were differentiated (45 s) in 0.15 % lithium carbonate diluted in distilled water and washed (90 s) with 70 % ethanol followed (30 s) with distilled water. The lithium carbonate, 70 % ethanol, and distilled water steps were repeated 2–5 times, until the sections showed blue myelin and pale gray nuclei. Sections were then incubated (25 min) in 0.1 % CV at 60 °C, washed with distilled water (30 s), differentiated (30 s) in 70 % ethanol, and finally dehydrated in a graded ethanol series, cleared in xylene, and cover slipped.

Immunohistochemical Staining

Immunohistochemistry was used to detect myelin (MBP, 1:200; Millipore), microglia (Iba1, 1:2000; Wako), astrocytes (GFAP, 1:2500; New England Biolabs), and neurofilament (NF, 1:250, Cell Signaling). For immunohistochemistry, sections were washed (30 min) with PB before starting and between each step. Sections were quenched (30 min) with 0.3 % H_2O_2 diluted in PB and underwent antigen retrieval (20 min) with 0.1 M pH 6.0 citrate buffer at 80 °C. Adjacent brain tissue sections were incubated with the appropriate primary antibody and normal goat serum (NGS; 1:100, Vector) in PB with 0.1 % Triton-X 100 (PBT) overnight at room temperature. Sections were incubated with the appropriate biotinylated secondary antibodies (1:500) and NGS (1:1000) in PBT for 1 h at room temperature and then with the avidin-biotin complex (Vectastain Elite ABC kit, Vector) diluted as per the manufacturer's instructions in PBT for 1 h. Sections were incubated in a solution containing 1.39 mM DAB diluted in PB. After 5 min, 0.3 % H_2O_2 was added to the DAB solution to a final concentration of 0.015 % for 3–5 min before final washes (3× 10 min) in 0.01 M pH 3.3 acetate buffer. Control experiments were performed where the primary antibody was omitted. Sections were mounted on glass slides, air dried, dehydrated in a graded series of ethanol (70–100 %), cleared in xylene, and cover slipped.

For NF staining, dried slides were counterstained with thionin to reveal cytoarchitecture, prior to cover slipping. Slides were dehydrated in a graded series of ethanol, cleared in xylene, and then rehydrated through the same series of ethanol and water. Sections were then stained (3 s) in an aqueous solution containing 1.7 M acetic acid, 0.36 M sodium hydroxide, and 0.125 % thionin (weight/volume) and rinsed twice in distilled water to remove excess stain. Sections were again dehydrated in the same graded series of ethanol, cleared in xylene, and cover slipped.

Radiosynthesis of BChE Ligand ^{123}I-PIP

Radiosynthesis of phenyl 4-[^{123}I]-iodophenylcarbamate (^{123}I-PIP) and its precursor phenyl 4-tributylstannylphenylcarbamate was

Table 1. Demographic data from healthy control (HC) and multiple sclerosis (MS) cases

Case	Age (years)	Sex	Diagnosis	Disease duration (years)	Postmortem interval (h)
HC-1	55	M	Normal	Not applicable	15
HC-2	63	F	Normal	Not applicable	23
HC-3	71	F	Normal	Not applicable	24
HC-4	61	F	Normal	Not applicable	20
HC-5	53	M	Normal	Not applicable	24
MS-1	50	M	SPMS	> 10	24
MS-2	64	F	SPMS	> 10	7
MS-3	66	F	SPMS	> 10	24
MS-4	64	M	PPMS	18	25
MS-5	63	F	SPMS	26	82

Table 2. Proportion of white matter lesions in a subset of MS sections that were visually identifiable by phenyl 4-[^{123}I]-iodophenylcarbamate (^{123}I-PIP) autoradiography

MS lesions	Frontal cortex ($n = 23$)	Occipital cortex ($n = 15$)
Visually identifiable (n (%))	20 (87)	12 (80)

carried out as previously described, with minor modifications [33]. The details are provided in the ESM.

Tissue Autoradiography

Using a modified method to detect cholinesterase activity in the AD brain [33], ^{123}I-PIP was evaluated for its ability to detect cholinesterase activity in normal and MS human orbitofrontal and occipital cortices. A subset of MS (MS1, MS2, and MS3) and healthy control (HC1, HC2, and HC3) tissues were used for this comparison. The details are provided in the ESM.

Lesion Classification and Analysis

Brain sections were systematically examined using brightfield microscopy, and lesions were identified. Lesions were classified by location in gray matter (juxtacortical, intracortical, and subpial) or white matter. Microglial activity patterns for each lesion were classified by way of Iba1 immunohistochemical staining, based on the method of Bö and Trapp into active, chronic active, and chronic inactive lesions [1]. For each lesion, AChE and BChE were classified qualitatively as having either decreased activity, no change, or increased activity compared with adjacent tissue. Serial tissue sections stained with GFAP and NF were used to qualitatively compare the microscopic appearance of AChE- and BChE-positive structures. Representative sections were imaged using a Zeiss Axio Scan.Z1 slide scanner with Zen 3.1 software (Blue Edition). Data was analyzed using Microsoft Excel and GraphPad Prism.

Lesion type (active, chronic active, and chronic inactive) was compared with BChE and AChE activity (decreased, no change, or increased), and X^2 goodness-of-fit test was carried out to establish a link between these two variables (GraphPad Prism).

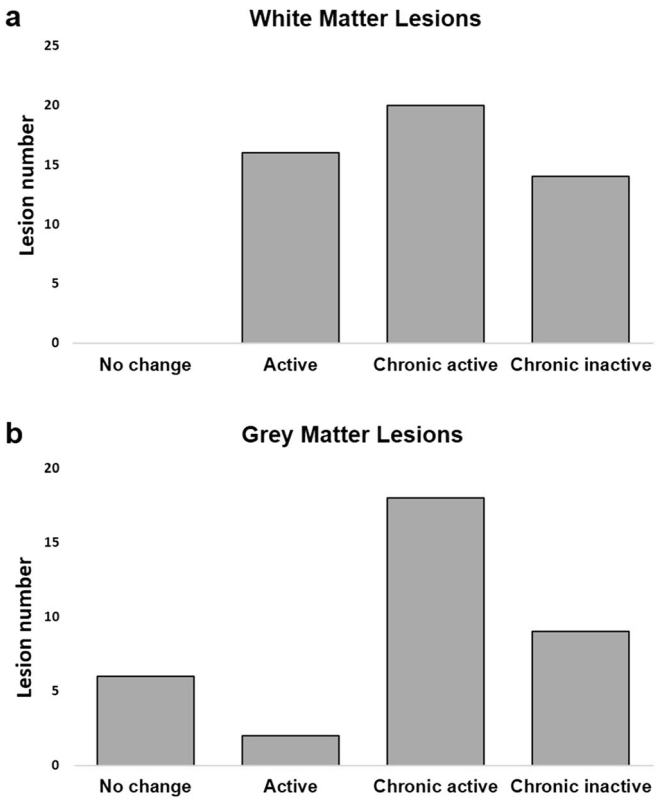

Fig. 1. Bar graphs representing the number of active, chronic active, and chronic inactive MS lesions in the white matter (**a**) and gray matter (**b**) using the Bö and Trapp lesion classification system [1].

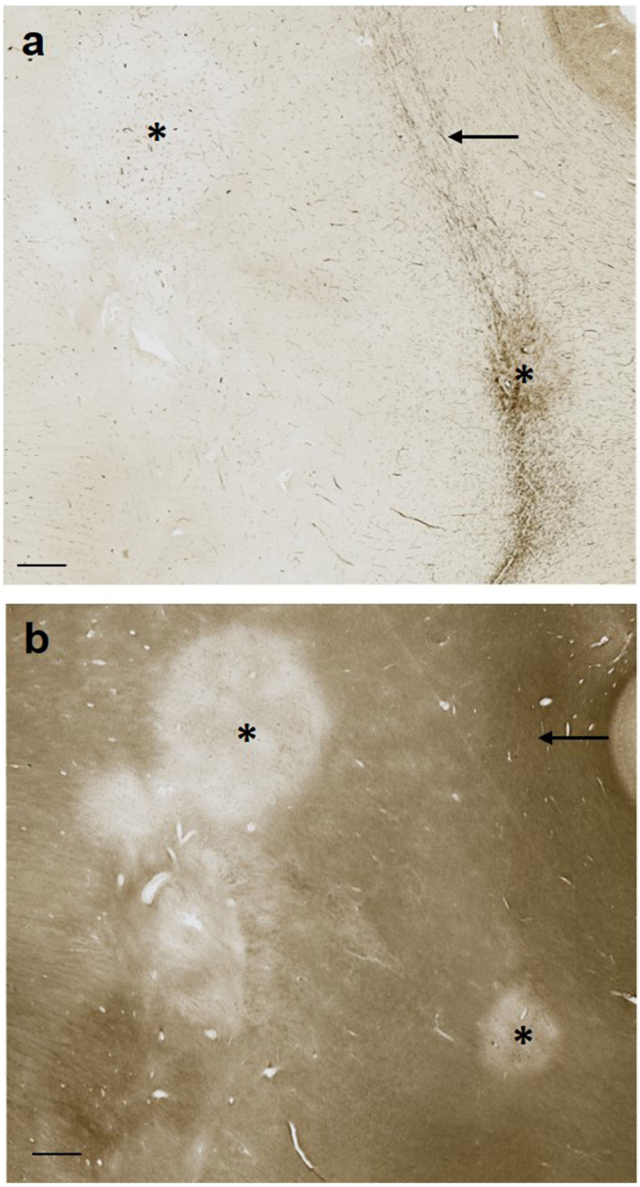

Fig. 2. A representative section of orbitofrontal white matter from an MS brain containing several chronic inactive demyelinating lesions (asterisks), comparing acetylcholinesterase (AChE) and butyrylcholinesterase (BChE) staining. **a** AChE staining shows increased activity within the lateral cholinergic projection (arrow) and subtle increased activity within one of the two demyelinating lesions (lower right asterisk). **b** BChE staining shows higher background activity in the white matter relative to AChE and no visualization of the lateral cholinergic projection. Demyelinating lesions are identified by loss of background BChE activity (asterisks), and no appreciable increase in BChE activity within these lesions is observed. Scale bars = 200 μm.

^{123}I-PIP activity was compared between normal and MS brain tissues by way of *in vitro* autoradiography. These images were qualitatively compared with adjacent brain tissue sections stained for cholinesterase activity, as well as MBP, Iba1, GFAP, and NF immunohistochemistry. Each MS autoradiogram was inspected visually, and it was determined for each lesion whether or not they could be identified (Table 2). Quantification of radioligand uptake in normal and MS tissues was done using PMOD (PMOD Technologies, V.4) imaging software and ImageJ (NIH open access, V.1.53a). Individual images were selected, regions of interest were manually outlined, and then a threshold was used to isolate the white matter. Average and standard deviations of the grayscale values were obtained for each section.

Results

Neuropathological Comparison of Healthy Control and MS Tissues

White matter of control brain tissue sections demonstrated uniform myelin staining, whereas MS tissue sections showed focal areas of patchy or complete loss of MBP staining demonstrating demyelination. In the gray matter, there was lighter uniform myelin staining in control brain tissue compared with areas of cortical demyelination in MS tissue. A total of 86 lesions were identified including 51 white matter and 35 cortical lesions (Fig. 1). A similar number of white matter lesions were observed between active, chronic active, and chronic inactive phenotypes (Fig. 1a). Comparatively, very few cortical lesions were active, with most lesions being chronic active or chronic inactive (Fig. 1b).

Distribution and Characteristics of AChE and BChE Activity in the Cortex and White Matter of Healthy Control and MS Tissues

In control brain tissue sections, AChE activity was localized to cortical pyramidal neurons as well as axons in the lateral cholinergic trajectory, and BChE activity was uniformly distributed throughout the white matter, with relatively lower activity in the gray matter as demonstrated previously [25]. In MS brain tissue, AChE was not appreciably different in the cortex or adjacent white matter but did show a faint increase in activity at the border of some demyelinated lesions (Fig. 2a). BChE activity was decreased compared to the background within demyelinated lesions and adjacent white matter (Fig. 2b), and in certain lesions, increased activity relative to the background was observed within the lesion rim and core. In general, increased BChE activity was associated with active and chronic active lesions, whereas chronic inactive lesions could show either increased or decreased BChE activity (Fig. 3a). The relationship between lesion type and BChE activity was found to be significant ($X^2 = 6.78$, $p < 0.05$), with active

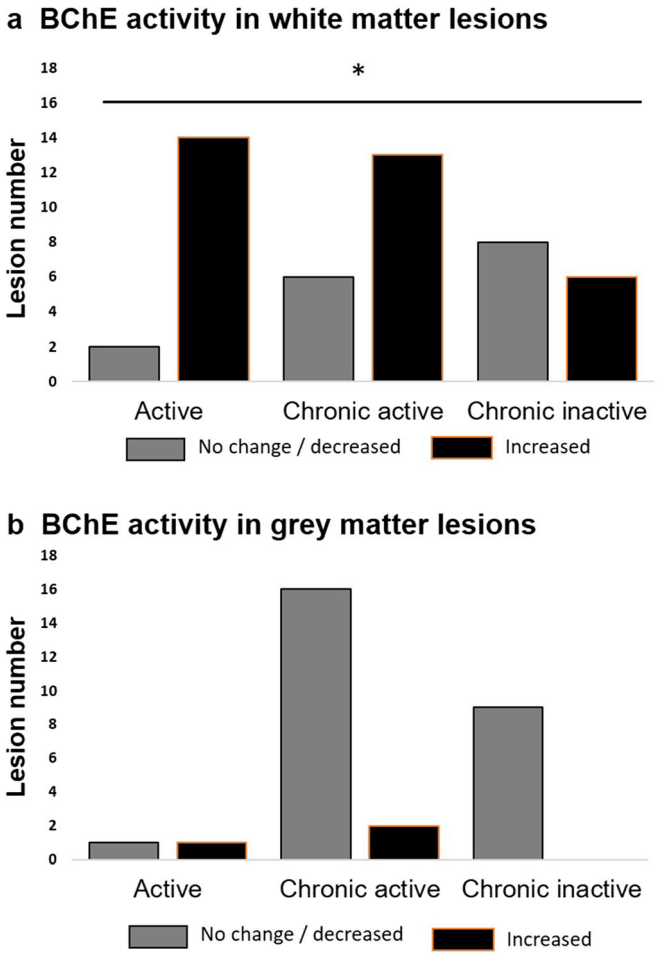

Fig. 3. Bar graphs comparing the combined number of MS lesions demonstrating no change, decreased, or increased butyrylcholinesterase (BChE) activity in the white matter and gray matter of MS brain tissue cases. **a** Within white matter lesions, there was a higher proportion of active and chronic active lesions with increased BChE activity ($^*X^2 = 6.78$, $p < 0.05$). **b** Within gray matter lesions, there was no difference in BChE activity based on lesion type.

lesions corresponding to increased BChE activity. There was no difference in BChE activity within cortical lesion types (Fig. 3b).

Upon examination of white matter lesions with increased BChE activity, the enzyme was observed within the lesion rim and core, on small blood vessels and cells with activated microglial morphology (Fig. 4a). In comparison, AChE activity was faintly increased within the lesion rim and core (Fig. 4b). The BChE activity pattern most closely resembled the Iba1-positive microglial staining pattern of adjacent tissue sections (Fig. 4c). In comparison, the increased AChE activity most closely resembled NF staining, suggesting exposed axon morphology (Fig. 4d).

Radiosynthesis of ^{123}I-PIP

^{123}I-PIP was synthesized, isolated from the reaction mixture using an HPLC method, and the combined HPLC fractions were concentrated to afford a 40 % non-decay-corrected radiochemical yield with a specific activity of 3400 GBq/μmol. The procedure was completed in 3 h. The data obtained during this procedure is consistent with previously described data for the synthesis of ^{123}I-PIP [33].

Human Tissue Autoradiography

Healthy control and MS brain tissues appeared undamaged following incubation with ^{123}I-PIP. In healthy control tissue, radioactivity accumulated uniformly in the white matter of orbitofrontal and occipital cortices, with more faint accumulation in the gray matter and around blood vessels (Fig. 5, top panel). In comparison, MS tissues showed accumulation of radioactivity in normal white matter and a lack of accumulation in white matter lesions (Fig. 5, bottom panel). Higher magnification views demonstrate focal areas where a lack of ^{123}I-PIP corresponds to MS lesions (Fig. 6),

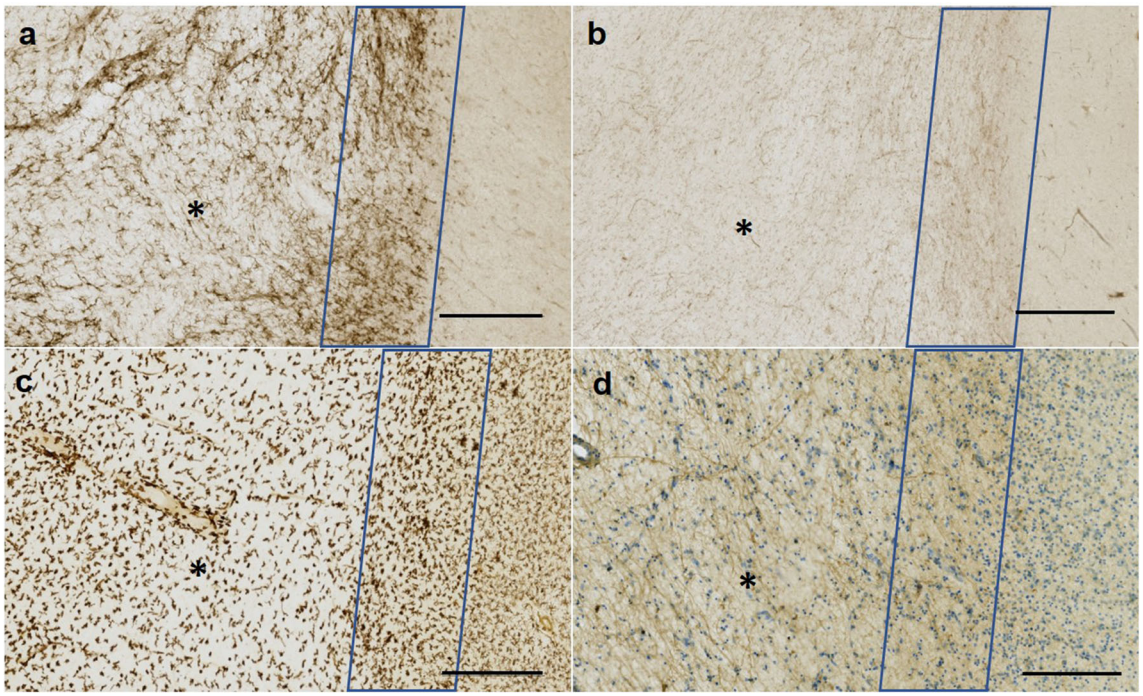

Fig. 4. Representative photomicrographs of a chronic active MS lesion, comparing adjacent sections stained for acetylcholinesterase (AChE) and butyrylcholinesterase (BChE) activity, and with Iba1 and neurofilament (NF) immunohistochemistry. The MS lesion rim is outlined by a blue box and the lesion core is denoted with an asterisk. **a** BChE histochemistry shows increased activity within the lesion core and rim, and normal activity in the adjacent white matter. **b** AChE histochemistry shows a faint increase in the lesion rim and core. **c** Iba1 immunohistochemistry shows increased microglial cellularity in the lesion rim and hypocellularity in the lesion core, characteristic of a chronic active lesion. **d** NF immunohistochemistry demonstrates exposed axons. The section is counterstained with thionin (blue) to show cells. Scale bars = 500 μm.

including active (Fig. 6b), chronic active (Fig. 6c, f, g, h), and chronic inactive (Fig. 6h).

A more detailed qualitative analysis of MS lesion visualization compared ^{123}I-PIP autoradiography with staining techniques for detecting microglia (Iba1), myelin (MBP), axons (NF), and cholinesterase activity. We observed decreased areas of radioactive accumulation corresponding to demyelinated white matter lesions. These same regions could show either increased or decreased BChE activity, and included active, chronic active, and chronic inactive lesions. Larger demyelinated chronic active and chronic inactive lesions, such as those represented in Figs. 5 and 6, were easily detectable by visual inspection. In total, 87 % of white matter lesions and 80 % of occipital lesions were identified by ^{123}I-PIP autoradiography (Table 2). The only lesions that were not identified visually using ^{123}I-PIP autoradiography included smaller lesions that were not demyelinated. NAWM did not show loss of myelination but did show changes to BChE activity with histochemical staining and ^{123}I-PIP autoradiography (Fig. 7). Quantification of radioligand uptake in normal and MS tissue was conducted using PMOD imaging software and ImageJ. However, the use of postmortem, formalin-fixed tissue presented a number of challenges for this analysis. The postmortem interval, time of tissue fixation, and length of tissue storage are all known factors to affect cholinesterase activity. With the number of cases available, it was not possible to control for these variables. In addition, slight differences in section thickness can affect radioligand uptake, and a standardized and unbiased method to delineate measuring area was not available. The results from this analysis were therefore not sufficiently robust and were excluded from this study. Future efforts will be made to develop a method which is appropriate for quantification of radioligand uptake in postmortem tissue.

Discussion

The present study is consistent with earlier reports that BChE activity is significantly altered in white matter lesions of people with MS [25]. In five MS brains examined, we have identified 86 lesions including 35 cortical and 51 white matter lesions. Within cortical gray matter lesions, there was a relatively low level of microglial activation despite extensive demyelination, consistent with historical neuropathological evaluations of MS brain tissue [3, 37–41]. Using correlative analysis, it was confirmed that within the white matter, increased BChE activity is associated with active lesions. This increased BChE activity appears to localize to small blood vessels and cells of activated

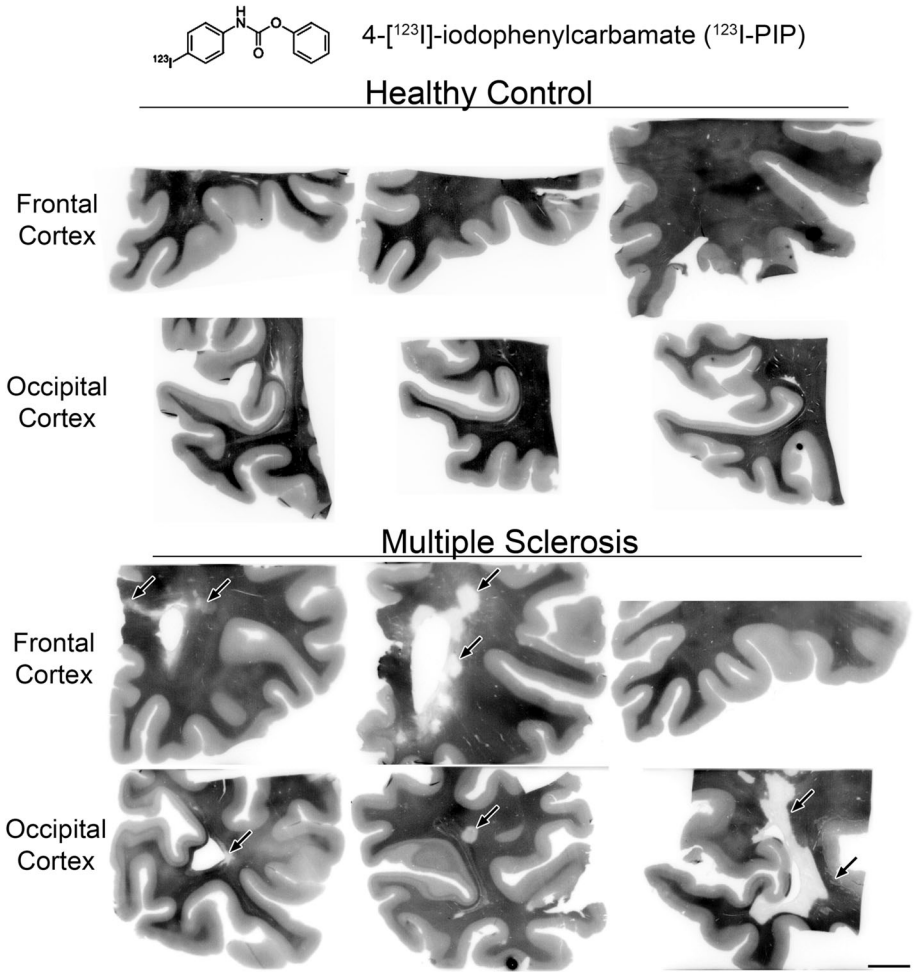

Fig. 5. Representative tissue sections comparing the distribution of phenyl 4-[^{123}I]-iodophenylcarbamate (^{123}I-PIP; chemical structure at the top) using *in vitro* autoradiography in healthy control and multiple sclerosis (MS) frontal (top row) and occipital (bottom row) cortex. In the healthy control tissue, ^{123}I-PIP accumulated uniformly in the white matter and accumulated faintly in the gray matter and around blood vessels. In the MS tissue, ^{123}I-PIP accumulated in the normal white matter, but did not accumulate in corresponding demyelinated MS lesions (arrows). ^{123}I-PIP had a specific activity of 3400 GBq/μmol (p. 3, ESM). Non-radioactive I-PIP was previously reported to have k_a values for both AChE (k_a $1.56 \pm 0.18 \times 10^4$ M^{-1} min^{-1}) and BChE (k_a $3.47 \pm 0.82 \times 10^2$ M^{-1} min^{-1}) [33]. Scale bar = 1 cm.

microglial morphology, consistent with previous reports. In comparison, AChE activity is faintly increased compared with the background of demyelinated white matter lesions, with no predilection for lesion type, and appears to morphologically resemble exposed axons. One limitation of this study, much like other postmortem studies in MS, is that our small study sample is comprised of subjects with long-standing, progressive forms of MS and thus does not accurately reflect the earlier, relapsing-remitting phase of the disease. Despite this, the presence of lesions containing activated microglia included in our sample allows for some degree of evaluation of the role of the cholinergic system in the immune response and highlights the need for better *in vivo* imaging technologies.

The association between myelin maintenance and BChE requires further evaluation. BChE activity is localized to white matter in human brain tissue and may decompact myelin through hydrolysis of long-chain acyl groups that anchor myelin proteins, such as PLP, to the cell membrane [34]. The integrity of these proteins is crucial for structural stability of myelin, and decompaction could expose sequestered myelin antigens to the immune system [34, 35, 42]. In addition to disruptions in myelin homeostasis, elevated BChE activity in microglia and in small blood vessels has several putative roles in contributing to the proinflammatory milieu observed in MS [43, 44]. This increase in glial BChE has been observed in experimental autoimmune encephalitis [45] and in postmortem MS brain tissue [25]. Elevated levels of serum and cerebrospinal fluid BChE correlate with decreased levels of ACh and increased pro-inflammatory cytokines [46]. A recent study examining AChE and BChE polymorphisms in MS showed that in healthy controls with

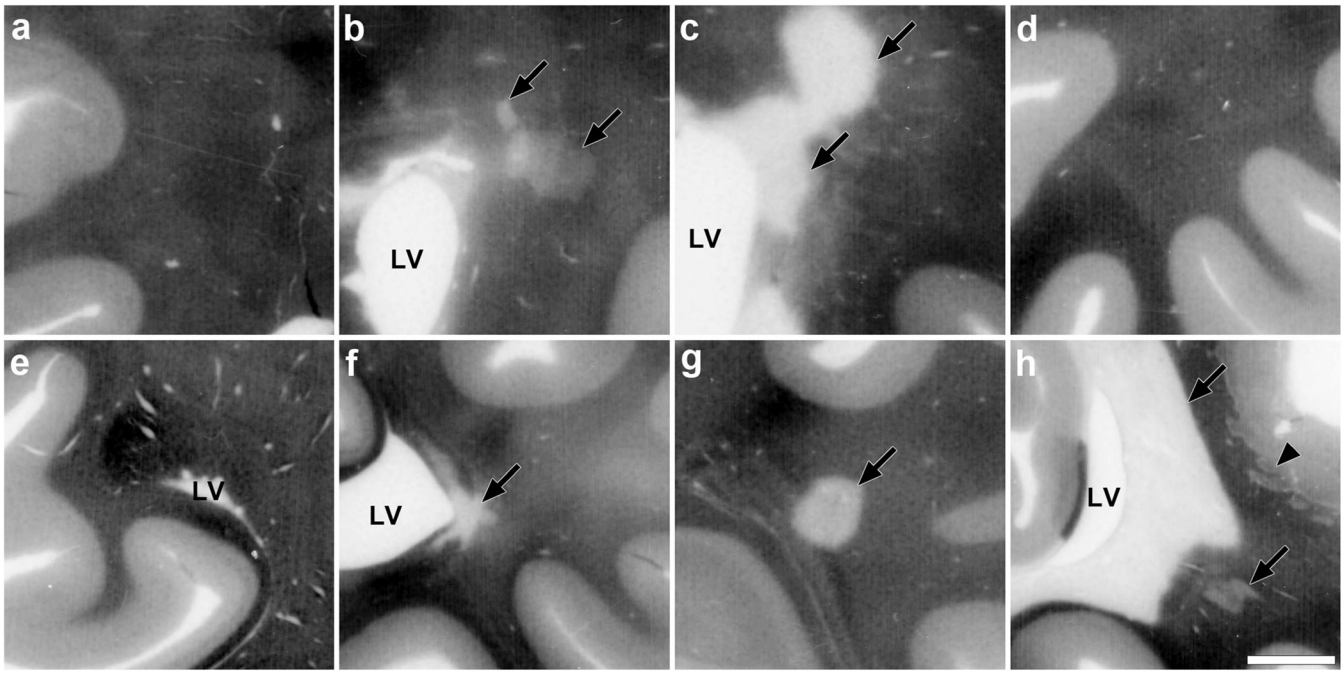

Fig. 6. Representative phenyl 4-[^{123}I]-iodophenylcarbamate (^{123}I-PIP) autoradiograms of human frontal (**a**–**d**) and occipital cortex (**e**–**h**) from a healthy control case (**a**, **e**) and three multiple sclerosis (MS) cases (**b**–**d**, **f**–**h**). The MS lesions highlighted here (arrows) were classified as follows: **b** active lesion, **c** chronic active lesion, **f** chronic active lesion, **g** chronic active lesion, and **h** large confluent periventricular chronic active lesion (upper arrow) and small, chronic inactive lesion (bottom right arrow) adjacent to a chronic inactive juxtacortical lesion (arrowhead). MS lesions were often associated with the lateral ventricle (LV). Arrows point to MS lesions; arrowhead points to MS lesion which extends into the gray matter. Scale bar = 5 mm.

the BChE-K allele, a genetic variant associated with a 30 % reduction in BChE activity, there was increased circulating ACh and decreased circulating pro-inflammatory cytokines [47]. MS subjects had a higher than expected frequency with the BChE-K allele, and those BChE-K-positive subjects had significantly higher levels of ACh-hydrolyzing activity that correlated with higher circulating pro-inflammatory cytokines, providing some of the only *in vivo* evidence for the deleterious role of BChE in MS [47].

It is well established that cholinergic neurotransmission is implicated in immunity by means of the cholinergic anti-inflammatory pathway and provides a means of communication between the CNS and end organs [48]. There is growing evidence supporting a broader role for the cholinergic anti-inflammatory pathway in maintaining the inflammatory milieu during normal conditions, and this becomes dysregulated in many neuroinflammatory conditions including MS [43]. In general, there is an age-related decrease in ACh signaling that is accentuated in neuroinflammatory disorders like MS, favoring an activated state for microglia [45, 49]. Although the specific role of BChE in modulating inflammation remains a matter of debate, increased BChE activity within activated glial cells likely acts in a deleterious manner, resulting in a decreased local concentration of ACh, thus attenuating the inhibitory effect on pro-inflammatory cytokine production by microglia.

In the present study, *in vitro* autoradiography using ^{123}I-PIP was able to accurately identify the pattern of myelin loss observed in white matter lesions in a subset of our MS tissue samples (MS1, MS2, and MS3), and allowed for visualization of microscopic abnormalities in the adjacent NAWM that corresponded to areas of altered BChE activity surrounding lesions. This observation requires validation using quantitative techniques. Traditional neuroimaging technologies, including MRI, have advanced our anatomical understanding of the brain, and remain the gold standard for the diagnosis and treatment monitoring of MS [9, 12]. PET and SPECT molecular imaging techniques rely on the ability of injected radiotracers to target specific ligands and accumulate into regions of high ligand concentration, in order to quantify the desired biochemical processes [50]. In MS, several radiotracers used experimentally in humans have allowed the *in vivo* evaluation of microglial activation; most notably, the 18-kDa translocator protein and several other molecular targets to study inflammation remain under investigation [51–53]. There have been radioligands developed for experimental use in neurodegenerative disorders targeted towards the cholinergic system [54, 55]. Notable among those include molecules that target vesicular acetylcholine transporter, AChE, nAChR, and mAChR [50, 56]. PIP, the compound used in the present study, was initially designed as a small-molecule SPECT imaging agent for

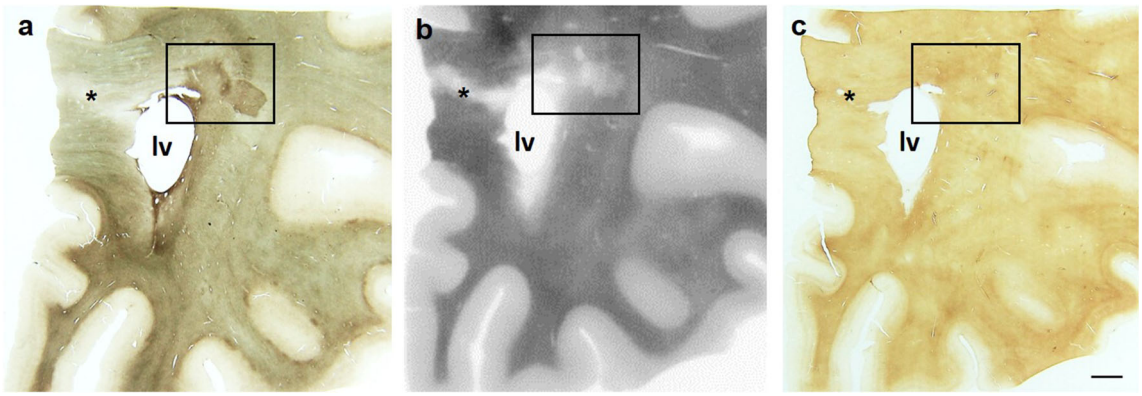

Fig. 7. Photomicrographs of representative serial sections from the orbitofrontal cortex of an MS case, comparing butyrylcholinesterase (BChE) staining (**a**), phenyl 4-[^{123}I]-iodophenylcarbamate (^{123}I-PIP) *in vitro* autoradiography (**b**), and myelin basic protein (MBP) staining (**c**). The box encompasses a small demyelinated active lesion contacting the lateral ventricle (lv) with two adjacent patches of microglial activation, consistent with normal-appearing white matter (NAWM) pathology, and the asterisks denote a partially remyelinated chronic active lesion. **a** BChE staining demonstrates heterogeneous activity within the white matter in the enclosed box, including increased activity within the demyelinated active lesion and in two larger patches of NAWM (box), and decreased BChE activity corresponding to the partially remyelinated chronic active lesion (asterisk). **b** ^{123}I-PIP *in vitro* autoradiography demonstrates altered radioactive accumulation within the active and chronic active lesions and NAWM, clearly distinguishing them from the surrounding white matter. **c** MBP staining shows focal areas of periventricular demyelination, without visualization of the corresponding NAWM regions. Scale bar = 5 mm.

research in AD due to its ability to bind to cholinesterase-associated β-amyloid plaques [29, 30, 33]. As the role of the cholinergic system in other neuroinflammatory disorders becomes more apparent, the applicability of these compounds is broadened and warrants further research. In MS, one potential utility of BChE imaging agents over existing microglial imaging agents would be the relatively high concentration of BChE in white matter that becomes increased in activated microglia and is also disrupted during demyelination. This unique property could, in turn, serve as a biomarker not only to track older demyelinated chronic inactive lesions where microglia are absent, but also to identify new disease activity in the NAWM. This remains an area of active interest. Given the ability to identify white matter lesions *in vitro* using autoradiography, the next step would be to assess the ability of ^{123}I-PIP and similar compounds *in vivo* in experimental MS animal models, with the end goal of using these as PET or SPECT imaging agents in MS patients to supplement current strategies for assessing demyelination and innate immune activation, and to improve diagnosis and treatment monitoring.

Conclusions

BChE imaging agents have the potential to detect MS lesions and subtle pathological changes in NAWM in postmortem MS tissue. Their potential utility in supplementing current imaging methods to facilitate early diagnosis and improved disease monitoring should be further investigated.

Author Contributions. MWDT: Acquisition, analysis, and interpretation of all data for this project. Drafting the work for publication. Critical revision and final approval of the manuscript.
MKC: Acquisition, analysis, and interpretation of histochemical data for this project. Critical revision and final approval of work.
GAR: Acquisition and analysis of radiochemistry data for this project. Critical revision and final approval of work.
DEB: Acquisition and analysis of radiochemistry data for this project. Final approval of work.
DL: Acquisition and analysis of data for this project. Final approval of work.
IRP: Conceived, designed, and performed the radiochemistry experiments. Aided in preparation, reviewing, and final approval the manuscript.
SD: Conceived and supervised the project. Facilitated writing of the manuscript and reviewed the manuscript. Final approval of the manuscript.

Funding. This work was supported in part by the Canadian Institutes of Health Research (PJT-153319), the Dalhousie Medical Research Foundation (DMRF Gillian's Hope Clinical Fellowship in MS Research, DMRF-Funded Chemists, the Durland Breakthrough Fund, and the DMRF Irene MacDonald Sobey Endowed Chair in Curative Approaches to Alzheimer's Disease), and the Dalhousie University Internal Medicine Research Fund.

Compliance with Ethical Standards

Conflict of Interest

M.W.D. Thorne reports grants from Dalhousie Medical Research Foundation and grants from Dalhousie University Internal Medicine Research Fund, during the conduct of the study.
M.K. Cash has nothing to disclose.
G.A. Reid has nothing to disclose.
D.E. Burley has nothing to disclose.
D. Luke has nothing to disclose.
I.R. Pottie reports grants from Canadian Institutes of Health Research, during the conduct of the study. In addition, Dr. Pottie has a patent WO 2014039526 licensed to Treventis Corp.
S. Darvesh reports grants from Canadian Institutes of Health Research (PJT-153319), grants from Dalhousie Medical Research Foundation Irene

MacDonald Sobey Endowed Chair in Curative Approaches to Alzheimer's Disease, grants from Dalhousie Medical Research Foundation (DMRF Gillian's Hope Clinical Fellowship in MS Research), grants from Dalhousie Medical Research Foundation (DMRF Chemists), grants from Dalhousie Medical Research Foundation (The Durland Breakthrough Fund), and grants from Dalhousie University Internal Medicine Research Fund, during the conduct of the study; non-financial support and others from Treventis Corporation, outside the submitted work. In addition, Dr. Darvesh has a patent International Publication Number WO 01/92240 issued, a US Patent no. 6436972 B1 issued, a US Patent no. 6544986 B2 issued, a patent International Publication Number WO 2010/025368 A1 issued, a New Zealand Patent no. 591824 issued, a European (Great Britain, France, and Germany) Patent no. 2320891 issued, a Hong Kong Patent no. HK1157227 issued, a US Patent no. 8795630 issued, a Japanese Patent no. 5734853 issued, an Australian Patent no. 2009285584 issued, a Canadian Patent no. 2735118 issued, an Israeli Patent Application no. 211347 issued, a Chinese Patent Application 200980137701.7 pending, a US provisional patent application Serial No. 61/736146 pending, a patent International Publication Number WO/2014/039526 pending, and a US provisional patent application Serial No. 62/884442 pending.

References

1. Bö L, Mörk S, Kong PA, Nyland H, Pardo CA, Trapp BD (1994) Detection of MHC class II-antigens on macrophages and microglia, but not on astrocytes and endothelia in active multiple sclerosis lesions. J Neuroimmunol 51:135–146
2. Bitsch A, Schuchardt J, Bunkowski S et al (2000) Acute axonal injury in multiple sclerosis. Correlation with demyelination and inflammation. Brain J Neurol 123(Pt 6):1174–1183
3. Kutzelnigg A, Lucchinetti CF, Stadelmann C, Brück W, Rauschka H, Bergmann M, Schmidbauer M, Parisi JE, Lassmann H (2005) Cortical demyelination and diffuse white matter injury in multiple sclerosis. Brain J Neurol 128:2705–2712
4. Gold R, Linington C, Lassmann H (2006) Understanding pathogenesis and therapy of multiple sclerosis via animal models: 70 years of merits and culprits in experimental autoimmune encephalomyelitis research. Brain J Neurol 129:1953–1971
5. Sanabria-Castro A, Flores-Díaz M, Alape-Girón A (2019) Biological models in multiple sclerosis. J Neurosci Res 00:1–18
6. Brownlee WJ, Miller DH (2014) Clinically isolated syndromes and the relationship to multiple sclerosis. J Clin Neurosci 21:2065–2071
7. Eran A, García M, Malouf R, Bosak N, Wagner R, Ganelin-Cohen E, Artsy E, Shifrin A, Rozenberg A (2018) MRI in predicting conversion to multiple sclerosis within 1 year. Brain Behav 8:e01042
8. Lublin FD (2014) New multiple sclerosis phenotypic classification. Eur Neurol 72(Suppl 1):1–5
9. Filippi M, Rocca MA, Ciccarelli O, de Stefano N, Evangelou N, Kappos L, Rovira A, Sastre-Garriga J, Tintorè M, Frederiksen JL, Gasperini C, Palace J, Reich DS, Banwell B, Montalban X, Barkhof F, MAGNIMS Study Group (2016) MRI criteria for the diagnosis of multiple sclerosis: MAGNIMS consensus guidelines. Lancet Neurol 15:292–303
10. Thompson AJ, Banwell BL, Barkhof F, Carroll WM, Coetzee T, Comi G, Correale J, Fazekas F, Filippi M, Freedman MS, Fujihara K, Galetta SL, Hartung HP, Kappos L, Lublin FD, Marrie RA, Miller AE, Miller DH, Montalban X, Mowry EM, Sorensen PS, Tintoré M, Traboulsee AL, Trojano M, Uitdehaag BMJ, Vukusic S, Waubant E, Weinshenker BG, Reingold SC, Cohen JA (2018) Diagnosis of multiple sclerosis: 2017 revisions of the McDonald criteria. Lancet Neurol 17:162–173
11. Wattjes MP, Rovira À, Miller D, Yousry TA, Sormani MP, de Stefano MP, Tintoré M, Auger C, Tur C, Filippi M, Rocca MA, Fazekas F, Kappos L, Polman C, Frederik Barkhof, Xavier Montalban, MAGNIMS study group (2015) Evidence-based guidelines: MAGNIMS consensus guidelines on the use of MRI in multiple sclerosis—establishing disease prognosis and monitoring patients. Nat Rev Neurol 11:597–606
12. Traboulsee A, Simon JH, Stone L, Fisher E, Jones DE, Malhotra A, Newsome SD, Oh J, Reich DS, Richert N, Rammohan K, Khan O, Radue EW, Ford C, Halper J, Li D (2016) Revised recommendations of the Consortium of MS Centers Task Force for a standardized MRI protocol and clinical guidelines for the diagnosis and follow-up of multiple sclerosis. AJNR Am J Neuroradiol 37:394–401
13. Filippi M, Preziosa P, Meani A, Ciccarelli O, Mesaros S, Rovira A, Frederiksen J, Enzinger C, Barkhof F, Gasperini C, Brownlee W, Drulovic J, Montalban X, Cramer SP, Pichler A, Hagens M, Ruggieri S, Martinelli V, Miszkiel K, Tintorè M, Comi G, Dekker I, Uitdehaag B, Dujmovic-Basuroski I, Rocca MA (2018) Prediction of a multiple sclerosis diagnosis in patients with clinically isolated syndrome using the 2016 MAGNIMS and 2010 McDonald criteria: a retrospective study. Lancet Neurol 17:133–142
14. Gaetani L, Prosperini L, Mancini A, Eusebi P, Cerri MC, Pozzilli C, Calabresi P, Sarchielli P, di Filippo M (2018) 2017 revisions of McDonald criteria shorten the time to diagnosis of multiple sclerosis in clinically isolated syndromes. J Neurol 265:2684–2687
15. Filippi M (2015) MRI measures of neurodegeneration in multiple sclerosis: implications for disability, disease monitoring, and treatment. J Neurol 262:1–6
16. De Santis S, Granberg T, Ouellette R et al (2019) Evidence of early microstructural white matter abnormalities in multiple sclerosis from multi-shell diffusion MRI. NeuroImage Clin 22:101699
17. Silver A (1974) The biology of cholinesterases. North-Holland Pub. Co.; American Elsevier Pub. Co., Amsterdam; New York
18. Li B, Stribley JA, Ticu A, Xie W, Schopfer LM, Hammond P, Brimijoin S, Hinrichs SH, Lockridge O (2000) Abundant tissue butyrylcholinesterase and its possible function in the acetylcholinesterase knockout mouse. J Neurochem 75:1320–1331
19. Mesulam M-M, Guillozet A, Shaw P, Quinn B (2002) Widely spread butyrylcholinesterase can hydrolyze acetylcholine in the normal and Alzheimer brain. Neurobiol Dis 9:88–93
20. Mesulam MM (2009) Acetylcholine neurotransmission in CNS. In: Squire LR (ed) Encyclopedia of neuroscience. Academic Press, Oxford, pp 1–4
21. Mesulam M-M, Mufson EJ, Levey AI, Wainer BH (1983) Cholinergic innervation of cortex by the basal forebrain: cytochemistry and cortical connections of the septal area, diagonal band nuclei, nucleus basalis (Substantia innominata), and hypothalamus in the rhesus monkey. J Comp Neurol 214:170–197
22. Selden NR, Gitelman DR, Salamon-Murayama N et al (1998) Trajectories of cholinergic pathways within the cerebral hemispheres of the human brain. Brain J Neurol 121(Pt 12):2249–2257
23. Darvesh S, Grantham DL, Hopkins DA (1998) Distribution of butyrylcholinesterase in the human amygdala and hippocampal formation. J Comp Neurol 393:374–390
24. Darvesh S, Hopkins DA (2003) Differential distribution of butyrylcholinesterase and acetylcholinesterase in the human thalamus. J Comp Neurol 463:25–43
25. Darvesh S, Leblanc AM, Macdonald IR et al (2010) Butyrylcholinesterase activity in multiple sclerosis neuropathology. Chem Biol Interact 187:425–431
26. Guillozet AL, Smiley JF, Mash DC, Mesulam MM (1997) Butyrylcholinesterase in the life cycle of amyloid plaques. Ann Neurol 42:909–918
27. Darvesh S, Hopkins DA, Geula C (2003) Neurobiology of butyrylcholinesterase. Nat Rev Neurosci 4:131–138
28. Ballard CG, Greig NH, Guillozet-Bongaarts AL, Enz A, Darvesh S (2005) Cholinesterases: roles in the brain during health and disease. Curr Alzheimer Res 2:307–318
29. Darvesh S (2013) Butyrylcholinesterase radioligands to image Alzheimer's disease brain. Chem Biol Interact 203:354–357
30. Darvesh S (2016) Butyrylcholinesterase as a diagnostic and therapeutic target for Alzheimer's disease. Curr Alzheimer Res 13:1173–1177
31. DeBay DR, Reid GA, Pottie IR et al (2017) Targeting butyrylcholinesterase for preclinical single photon emission computed tomography (SPECT) imaging of Alzheimer's disease. Alzheimers Dement N Y N 3:166–176
32. DeBay DR, Pottie I, Reid AG et al (2019) P2-402 [abstract]: Synthesis and in vivo brain pet evaluation of 1-methyl-4-piperidyl p-18[f]flourobenzoate (trv6501): a butyrylcholinesterase-specific radioligand for Alzheimer's disease. Alzheimer's Association

International Conference 2019, Los Angeles, CA. Alzheimers Dement 15:P760
33. Macdonald IR, Reid GA, Pottie IR et al (2016) Synthesis and preliminary evaluation of phenyl 4-123I-iodophenylcarbamate for visualization of cholinesterases associated with Alzheimer disease pathology. J Nucl Med 57:297–302
34. Pottie IR, Higgins EA, Blackman RA, Macdonald IR, Martin E, Darvesh S (2011) Cysteine thioesters as myelin proteolipid protein analogues to examine the role of butyrylcholinesterase in myelin decompaction. ACS Chem Neurosci 2:151–159
35. Caprariello AV, Rogers JA, Morgan ML, Hoghooghi V, Plemel JR, Koebel A, Tsutsui S, Dunn JF, Kotra LP, Ousman SS, Wee Yong V, Stys PK (2018) Biochemically altered myelin triggers autoimmune demyelination. Proc Natl Acad Sci 115:5528–5533
36. Macdonald IR, Maxwell SP, Reid GA, Cash MK, DeBay DR, Darvesh S (2017) Quantification of butyrylcholinesterase activity as a sensitive and specific biomarker of Alzheimer's disease. J Alzheimers Dis 58:491–505
37. Bø L, Vedeler CA, Nyland H, Trapp BD, Mørk SJ (2003) Intracortical multiple sclerosis lesions are not associated with increased lymphocyte infiltration. Mult Scler Houndmills Basingstoke Engl 9:323–331
38. Lassmann H, Brück W, Lucchinetti CF (2007) The immunopathology of multiple sclerosis: an overview. Brain Pathol 17:210–218
39. Calabrese M, Filippi M, Gallo P (2010) Cortical lesions in multiple sclerosis. Nat Rev Neurol 6:438–444
40. Calabrese M, Magliozzi R, Ciccarelli O, Geurts JJG, Reynolds R, Martin R (2015) Exploring the origins of grey matter damage in multiple sclerosis. Nat Rev Neurosci 16:147–158
41. Prins M, Schul E, Geurts J, van der Valk P, Drukarch B, van Dam AM (2015) Pathological differences between white and grey matter multiple sclerosis lesions. Ann N Y Acad Sci 1351:99–113
42. Duncan ID, Hammang JP, Goda S, Quarles RH (1989) Myelination in the jimpy mouse in the absence of proteolipid protein. Glia 2:148–154
43. Di Bari M, Di Pinto G, Reale M et al (2017) Cholinergic system and neuroinflammation: implication in multiple sclerosis. Cent Nerv Syst Agents Med Chem 17:109–115
44. Hoover DB (2017) Cholinergic modulation of the immune system presents new approaches for treating inflammation. Pharmacol Ther 179:1–16
45. Di Pinto G, Di Bari M, Martin-Alvarez R et al (2018) Comparative study of the expression of cholinergic system components in the CNS of experimental autoimmune encephalomyelitis mice: acute vs remitting phase. Eur J Neurosci 48:2165–2181
46. Reale M, de Angelis F, di Nicola M, Capello E, di Ioia M, Luca G, Lugaresi A, Tata A (2012) Relation between pro-inflammatory cytokines and acetylcholine levels in relapsing-remitting multiple sclerosis patients. Int J Mol Sci 13:12656–12664
47. Reale M, Costantini E, Di Nicola M et al (2018) Butyrylcholinesterase and acetylcholinesterase polymorphisms in multiple sclerosis patients: implication in peripheral inflammation. Sci Rep 8:1319
48. Pavlov VA, Tracey KJ (2006) Controlling inflammation: the cholinergic anti-inflammatory pathway. Biochem Soc Trans 34:1037–1040
49. Di Bari M, Reale M, Di Nicola M et al (2016) Dysregulated homeostasis of acetylcholine levels in immune cells of RR-multiple sclerosis patients. Int J Mol Sci 17(12):2009
50. Bauckneht M, Capitanio S, Raffa S, Roccatagliata L, Pardini M, Lapucci C, Marini C, Sambuceti G, Inglese M, Gallo P, Cecchin D, Nobili F, Morbelli S (2019) Molecular imaging of multiple sclerosis: from the clinical demand to novel radiotracers. EJNMMI Radiopharm Chem 4(1):6
51. Rissanen E, Tuisku J, Rokka J et al (2014) In vivo detection of diffuse inflammation in secondary progressive multiple sclerosis using PET imaging and the radioligand ^{11}C-PK11195. J Nucl Med 55:939–944
52. Datta G, Colasanti A, Kalk N et al (2017) 11C-PBR28 and 18F-PBR111 detect white matter inflammatory heterogeneity in multiple sclerosis. J Nucl Med 58:1477–1482
53. Högel H, Rissanen E, Vuorimaa A, Airas L (2018) Positron emission tomography imaging in evaluation of MS pathology in vivo. Mult Scler J 24:1399–1412
54. Bohnen NI, Grothe MJ, Ray NJ, Müller MLTM, Teipel SJ (2018) Recent advances in cholinergic imaging and cognitive decline-revisiting the cholinergic hypothesis of dementia. Curr Geriatr Rep 7:1–11
55. Bohnen NI, Kanel P, Müller MLTM (2018) Molecular imaging of the cholinergic system in Parkinson's disease. Int Rev Neurobiol 141:211–250
56. Roy R, Niccolini F, Pagano G, Politis M (2016) Cholinergic imaging in dementia spectrum disorders. Eur J Nucl Med Mol Imaging 43:1376–1386